

# Indifference to Hydrogen Bonding in a Family of Secondary Amides

D. Tyler McQuade, Sonya L. McKay, Douglas R. Powell, and Samuel H. Gellman\*

Contribution from the Department of Chemistry, University of Wisconsin, Madison, Wisconsin 53706

Received April 7, 1997<sup>⊗</sup>

**Abstract:** N–H stretch region IR spectroscopy has been used to probe the hydrogen bond-donating properties of six structurally related secondary amides in which the amide group is flanked by sterically bulky groups. For three of the compounds, solid state IR analysis reveals N–H stretch bands  $>3400\text{ cm}^{-1}$ , which suggests the absence of intermolecular N–H–O=C hydrogen bonds. Crystallographic data for these three amides confirm the absence of a standard N–H–O=C interaction. For the other three amides, N–H stretch bands in the range  $3370\text{--}3290\text{ cm}^{-1}$  suggest the occurrence of intermolecular N–H–O=C hydrogen bonds in the solid state, but high quality crystals could not be grown. Steric hindrance to hydrogen bond donation by these amides is manifested in IR data obtained in DMSO: although this solvent is a strong hydrogen bond acceptor, N–H stretch bands are observed for both solvent-hydrogen bonded and non-hydrogen bonded amide groups. The amides described here and related compounds should be useful for calibrating spectroscopic methods that are intended to detect hydrogen bond formation.

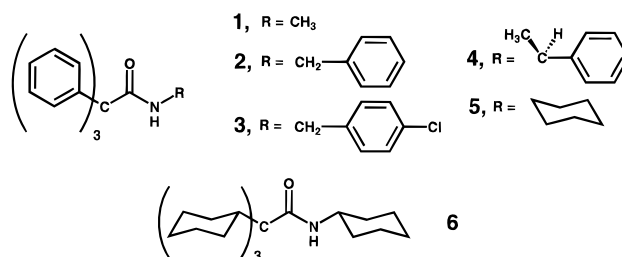
## Introduction

Hydrogen bonds are widely viewed to be determinants of crystal packing arrangements, biopolymer folding and complexation behavior, host–guest selectivities, and other noncovalently controlled phenomena.<sup>1</sup> Detection of hydrogen bonds is therefore of general interest. When high-resolution structural data are available, from crystallography or NMR spectroscopy, hydrogen bonds are conventionally identified via geometric criteria (interatomic distances, and angular relationships among the donor and acceptor groups).<sup>2</sup> Various spectroscopic parameters associated with donor and/or acceptor groups may also provide information on the existence of hydrogen bonds, and these parameters can often be obtained even when high-resolution structural data are unavailable. IR spectroscopy has the longest history as a tool for hydrogen bond detection, but other types of spectroscopy have also been employed for this purpose.<sup>2</sup>

The present study arose from our interest in reports by Triggs et al.,<sup>3,4</sup> who used Raman and preresonant Raman spectroscopic data to conclude that a variety of simple secondary amides are not hydrogen bonded in the solid state. (The secondary amide unit is a subject of particular interest because of its occurrence in peptides and proteins.) We reexamined one of the compounds in question, and pointed out that N–H stretch region IR data in this case are fully consistent with hydrogen bonding in the

solid state.<sup>5</sup> We therefore suggested that variations in the Raman data arise from subtle differences among hydrogen bonding interactions, rather than from the presence or absence of hydrogen bonding.

To calibrate the Raman method, and other methods, with regard to secondary amide hydrogen bond detection in the solid state, it is necessary to have crystalline amides that do not form hydrogen bonds. This situation is unusual, since the secondary amide unit has a donor group (amide proton) and an acceptor group (carbonyl), and hydrogen bond formation is usually maximized in the solid state.<sup>1a</sup> Here we describe a set of secondary amides, **1–6**, that contain sterically bulky hydrocar-



bon fragments near the hydrogen bonding sites. A combination of IR and crystallographic data indicates that hydrogen bonding is not obligatory within this family of molecules, either in the solid state or in a strongly hydrogen bonding solvent.

## Results and Discussion

**N–H Stretch IR Data.** Table I summarizes the positions of the amide N–H stretch bands for **1–6** under three conditions: in the solid state (KBr pellet); in  $\text{CHCl}_3$ , a solvent that is not a conventional hydrogen bond acceptor; and in DMSO, a solvent that is a strong hydrogen bond acceptor. Extensive precedent indicates that secondary amide N–H groups engaged in standard amide–amide hydrogen bonds ( $\text{C}=\text{O}\cdots\text{H}-\text{N}$ ) display stretch bands in the range  $3370\text{--}3250\text{ cm}^{-1}$ .<sup>6</sup> Secondary amide N–H groups free of hydrogen bonding are characterized by stretch bands in the range  $3500\text{--}3400\text{ cm}^{-1}$ .<sup>6</sup> The N–H

<sup>⊗</sup> Abstract published in *Advance ACS Abstracts*, August, 15, 1997.

(1) For leading references, see: (a) Etter, M. C. *Acc. Chem. Res.* **1990**, 23, 120. (b) Jeffrey, G. A.; Saenger, W. *Hydrogen Bonding in Biological Structures*; Springer-Verlag: Berlin, 1991. (c) Hollingsworth, M. D.; Brown, M. E.; Hillier, A. C.; Santarsiero, B. D.; Chaney, J. D. *Science* **1996**, 273, 1355. (d) Brunet, P.; Simard, M.; Wuest, J. D. *J. Am. Chem. Soc.* **1997**, 119, 2737.

(2) For leading references, see: (a) Pimentel, G. C.; McClellan, A. L. *The Hydrogen Bond*; Freeman: San Francisco, 1960. (b) Hamilton, W. C.; Ibers, J. A. *Hydrogen Bonding in Solids*; W. A. Benjamin: Reading, MA, 1968. (c) Pimentel, G. C.; McClellan, A. L. *Annu. Rev. Phys. Chem.* **1971**, 347. (d) Aaron, H. S. *Top. Stereochem.* **1980**, 11, 1. (e) Taylor, R.; Kennard, O.; Versichel, W. *Acta Crystallogr.* **1984**, B40, 280. (f) Held, A.; Pratt, D. W. *J. Am. Chem. Soc.* **1993**, 115, 9708, 9718. (g) Gu, Z.; Zambrano, R.; McDermott, A. *J. Am. Chem. Soc.* **1994**, 116, 6368.

(3) Triggs, N. E.; Bonn, R. T.; Valentini, J. J. *J. Phys. Chem.* **1993**, 97, 5535.

(4) Triggs, N. E.; Valentini, J. J. *Isr. J. Chem.* **1994**, 34, 89.

(5) Skwierczynski, R. D.; Gellman, S. H. *J. Phys. Chem.* **1994**, 98, 3694.

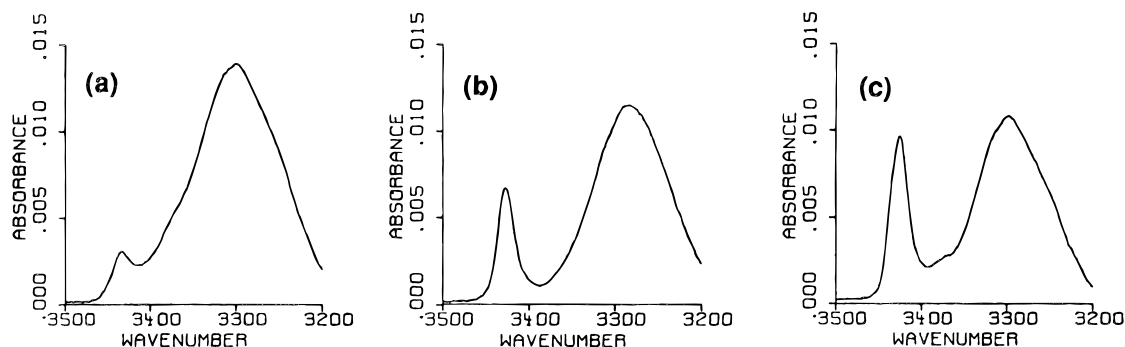


**Figure 1.** N–H stretch region FT-IR data for 10 mM amide samples in DMSO at room temperature, after subtraction of the spectrum of pure DMSO: (a) **2**, maxima at 3434 and 3302  $\text{cm}^{-1}$ ; (b) **4**, maxima at 3428 and 3285  $\text{cm}^{-1}$ ; and (c) **5**, maxima at 3426 and 3298  $\text{cm}^{-1}$ .

**Table 1.** N–H Stretch Band Positions ( $\text{cm}^{-1}$ ) for Amides **1–6** in  $\text{CHCl}_3$  Solution and in the Solid State (KBr pellet) and for amides **1–5** in DMSO Solution

	DMSO (major)	DMSO (minor)	KBr	$\text{CHCl}_3$
<b>1</b>	3315	3449	3446	3449
<b>2</b>	3302	3434	3292	3432
<b>3</b>	3293	3432	3371	3432
<b>4</b>	3285	3428	3417	3427
<b>5</b>	3298	3426	3373	3424
<b>6</b>			3417	3462

stretch band of *N*-ethylacetamide in the gas phase, for example, occurs at 3472  $\text{cm}^{-1}$ .<sup>6a</sup> Also found in this range are stretch bands for N–H groups engaged in interactions that may correspond to weak hydrogen bonds. *N*-Ethylacetamide displays an N–H stretch band at 3452  $\text{cm}^{-1}$  in dilute  $\text{CHCl}_3$  solution and at 3442  $\text{cm}^{-1}$  in dilute  $\text{C}_6\text{H}_6$  solution.<sup>6a</sup> The 20  $\text{cm}^{-1}$  shift to lower energy in  $\text{CHCl}_3$  relative to the gas phase may be attributed to weak N–H–Cl hydrogen bonding, and the further 10  $\text{cm}^{-1}$  shift to lower energy in benzene may be attributed to hydrogen bonding between N–H and the  $\pi$ -electron system of the aromatic ring.<sup>7</sup>

In dilute  $\text{CHCl}_3$  solution, amides **1–6** display N–H stretch bands between 3420 and 3470  $\text{cm}^{-1}$ . Each of these bands arises from N–H free of strong hydrogen bonding interactions. The band observed for **1** is similar in position to the band reported for dilute *N*-ethylacetamide in  $\text{CHCl}_3$ .<sup>6a</sup> The bands for **2–5** are 17–25  $\text{cm}^{-1}$  lower in energy than the band for **1**. These shifts to lower energy arise at least in part from the greater steric bulk of the *N*-alkyl groups of **2–5** relative to the *N*-methyl group of **1**.<sup>6c</sup> (*N*-Methylacetamide, for example, displays an N–H stretch band at 3460  $\text{cm}^{-1}$  in dilute  $\text{CH}_2\text{Cl}_2$ , while the analogous band of *N*-1-adamantylacetamide occurs at 3430  $\text{cm}^{-1}$ .<sup>6f</sup>) Fully saturated amide **6** displays the highest energy N–H stretch band in dilute  $\text{CHCl}_3$  solution, ca. 38  $\text{cm}^{-1}$  above the N–H stretch

band of the closest structural analogue, **5**. One possible explanation for the unique position of the N–H stretch band of **6** is that increased steric bulk around the amide group, resulting from replacement of phenyl groups by cyclohexyl groups, inhibits weak hydrogen bonding between N–H and  $\text{CHCl}_3$  molecules. A second possible explanation for the position of the N–H stretch band of **6** is that there is some degree of intramolecular N–H– $\pi$  hydrogen bonding involving the triphenylmethane moiety common to **1–5** (this point is discussed further below). These two explanations are not exclusive of one another.

In dilute DMSO solution, amides **1–5** display two bands in the N–H stretch region (**6** was insoluble in DMSO). In all cases, the minor band occurs at the same position as the single N–H stretch band observed in  $\text{CHCl}_3$  (within the nominal 2- $\text{cm}^{-1}$  resolution of these measurements), indicating that this minor band in DMSO arises from unsolvated N–H. These observations are remarkable, since secondary amides typically display only a hydrogen bonded N–H stretch in dilute DMSO solution (*N*-methylacetamide in dilute DMSO solution, for example, displays a band at 3300  $\text{cm}^{-1}$ , but no band between 3400 and 3500  $\text{cm}^{-1}$ ). The major N–H stretch bands occur in the range 3315–3285  $\text{cm}^{-1}$  for **1–5** in DMSO, as expected for N–H–O=S(CH<sub>3</sub>)<sub>2</sub> hydrogen bonding.

Figure 1 shows N–H stretch region IR data for **2**, **4**, and **5** in DMSO, to illustrate the effect of varying the *N*-alkyl substituent on the proportions of solvated and unsolvated N–H bands. The corresponding spectra for **1** and **3** are qualitatively similar to the one shown for **2** in that the unsolvated N–H stretch band is very small. The increased proportion of the unsolvated form observed for **4** and **5** relative to **1–3** presumably results from the fact that **4** and **5** have an alkyl branch point directly adjacent to the amide nitrogen, and this branching sterically hinders N–H–O=S(CH<sub>3</sub>)<sub>2</sub> hydrogen bonding. The amide I bands, which have a large component of C=O stretching, are indistinguishable in  $\text{CHCl}_3$  and DMSO for **1–5** (data not shown).

In the solid state, only **1** displays an N–H stretch band at the same position as observed in  $\text{CHCl}_3$ ; the solid state N–H stretch bands of **2–6** are 10–140  $\text{cm}^{-1}$  lower in energy than the analogous bands in  $\text{CHCl}_3$ . For three of these amides, **2**, **3** and **5**, the positions of the N–H stretch bands suggest that intermolecular amide–amide hydrogen bonding occurs in the solid state. For the other three amides, **1**, **4**, and **6**, the N–H stretch bands are  $>3400$   $\text{cm}^{-1}$ , which indicates that conventional N–H–O=C hydrogen bonds do *not* occur in the solid state. High-quality crystals could be grown for each of these latter three amides (but not, despite repeated attempts, for **2**, **3**, or **5**), and the X-ray structures confirmed the absence of conventional amide–amide hydrogen bonds in the solid state.

(6) For leading references, see: (a) Klemperer, W.; Cronyn, M. W.; Maki, A. H.; Pimentel, G. C. *J. Am. Chem. Soc.* **1954**, *76*, 5846. (b) Tsuboi, M.; Shimanouchi, T.; Mizushima, S. *J. Am. Chem. Soc.* **1959**, *81*, 1406. (c) Boussard, G.; Marraud, M. *J. Am. Chem. Soc.* **1985**, *107*, 1825. (d) Maxfield, F. R.; Leach, S. J.; Stimson, E. R.; Powers, S. P.; Scheraga, H. A. *Biopolymers* **1979**, *18*, 2507. (e) Gellman, S. H.; Dado, G. P.; Liang, G.-B.; Adams, B. R. *J. Am. Chem. Soc.* **1991**, *113*, 1164. (f) Dado, G. P.; Gellman, S. H. *J. Am. Chem. Soc.* **1993**, *115*, 4228.

(7) (a) Krishnamurty, G. V. G.; Subrahmanyam, B. *Proc. Indian Acad. Sci.* **1982**, *91*, 57. (b) Nikolic, A. D.; Tarjani, M.; Perisic-Janjic, M.; Petrovic, S. D. *J. Mol. Struct.* **1988**, *174*, 129. (c) Gallo, E. A.; Gellman, S. H. *Tetrahedron Lett.* **1992**, *33*, 7485. (d) Viswamitra, M. A.; Radhakrishnan, R.; Bandekar, J.; Desiraju, G. R. *J. Am. Chem. Soc.* **1993**, *115*, 4868. This study includes a statistical analysis of NH– $\pi$  and OH– $\pi$  hydrogen bonds in the Cambridge Structural Database. The authors conclude that such hydrogen bonds are “energetically and structurally significant”, although the data themselves suggest that such interactions are rare and probably represent NH/ $\pi$  or OH/ $\pi$  juxtapositions that result from other packing forces. (e) Adams, H.; Harris, K. D. M.; Hembury, G. A.; Hunter, C. A.; Livingstone, D.; McCabe, J. F. *J. Chem. Soc., Chem. Commun.* **1996**, 2531.

**Table 2.** Geometrical Parameters for N–H–O=C Units with the Shortest Intermolecular H–O Distance in the Crystals of Amides **1**, **4**, and **6**

	O···H, Å	N···O, Å	angle at H, deg	angle at O, deg	out-of-plane angle, <sup>a</sup> deg
<b>1</b>	5.136(12)	4.562(12)	45.5(9)	148.3(9)	68.6(9)
<b>4</b>	6.417(6)	6.271(6)	76.6(3)	130.3(3)	36.1(3)
<b>6</b>	2.673(1)	3.292(1)	128.26(3)	155.8(2)	14.0(2)

<sup>a</sup> Angle between the planes defined by C=O···H and N–C=O of the hydrogen-bond-acceptor amide.

**Table 3.** Data Collection and Refinement for Amides **1**, **4**, and **6**

	<b>1</b>	<b>4</b>	<b>6</b>
formula	C <sub>21</sub> H <sub>19</sub> NO	C <sub>28</sub> H <sub>25</sub> NO	C <sub>26</sub> H <sub>45</sub> NO
MW	301.37	391.49	387.63
cryst size, mm	0.2 × 0.2 × 0.2	0.6 × 0.4 × 0.1	0.52 × 0.18 × 0.14
cryst syst	orthorhombic	orthorhombic	triclinic
space group	<i>Pbcn</i>	<i>P2<sub>1</sub>2<sub>1</sub>2<sub>1</sub></i>	<i>P1</i>
<i>a</i> , Å	14.1730(4)	8.9722(2)	10.6895(2)
<i>b</i> , Å	7.2910(2)	9.8641(2)	12.1387(3)
<i>c</i> , Å	30.0450(5)	24.0202(5)	18.7127(4)
α, deg	90	90	90.815(2)
β, deg	90	90	103.114(2)
γ, deg	90	90	94.059(2)
vol, Å <sup>3</sup>	3104.71(13)	2125.85(8)	2357.70(9)
<i>Z</i>	8	4	4
<i>D</i> <sub>calcd</sub> , g/cm <sup>3</sup>	1.289	1.223	1.092
<i>F</i> (000)	1280	832	864
μ, mm <sup>-1</sup>	0.079	0.073	0.064
temp, K	133(2)	133(2)	133(2)
θ range, deg	1.36–26.17	1.70–25.95	2.47–29.03
scan range, deg	0.3 in φ	0.3 in φ	0.4 in φ
no. of reflns collected	12045	8319	25537
no. of unique reflns	2586	3670	11120
<i>R</i> <sub>merg</sub>	0.0731	0.0282	0.0304
no. of reflns obsd	1956	3417	8007
<i>R</i> ( <i>F</i> )	0.0659	0.0314	0.0459
<i>wR</i> ( <i>F</i> <sup>2</sup> )	0.1333	0.0797	0.1172
<i>S</i>	1.265	1.082	1.029
Δρ <sub>max/min</sub> , e/Å <sup>3</sup>	0.239/–0.231	0.164/–0.143	0.314/–0.276
data:param ratio	12.4:1	13.5:1	22.0:1

**Crystal Structures.** Table 2 provides geometrical parameters for the shortest intermolecular NH···O contacts between neighboring molecules in the crystal structures of **1**, **4**, and **6**, and Table 3 provides crystallographic information. Figure 2 shows the appropriate pair of molecules for **1**, with the relevant atoms labeled. Figures 3 and 4 show the analogous neighboring pairs for **4** and **6**. An O–H separation of 2.4 Å, slightly less than the sum of the oxygen and hydrogen van der Waals radii, is commonly taken as an upper limit for identifying O–H hydrogen bonds in crystallographic data.<sup>2e</sup> For **1** and **4**, the nearest neighbor NH···O contacts are far larger than this limiting value (>5 Å in both cases), clearly indicating that there is no amide–amide hydrogen bonding in these crystals. For **6**, the NH···O separation is 2.67 Å, which is only modestly larger than the conventional cutoff value. Thus, there may be a weak NH···O attraction in crystalline **6**. IR data support this possibility, since the N–H stretch band of solid **6** is 45 cm<sup>-1</sup> lower than that N–H stretch band for **6** in CHCl<sub>3</sub> solution. However, by both IR and geometric criteria, the NH···O interaction in crystalline **6** does not correspond to a conventional amide–amide hydrogen bond.

Amide N–H units can form weak hydrogen bonds with π-electrons of multiple carbon–carbon bonds, including aro-

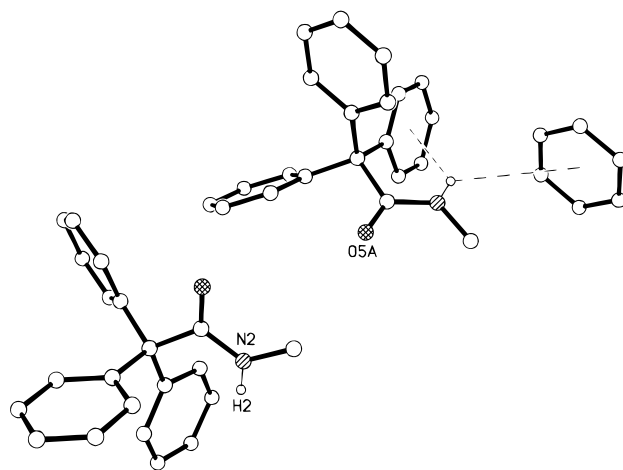


**Figure 2.** Ball-and-stick representation of the neighboring pair of molecules in crystalline **1** with the shortest intermolecular NH···O separation (geometrical parameters may be found in Table 2). The atoms in question are labeled. The dotted lines indicate the shortest intramolecular and intermolecular NH···O (centroid) contacts in the crystal.

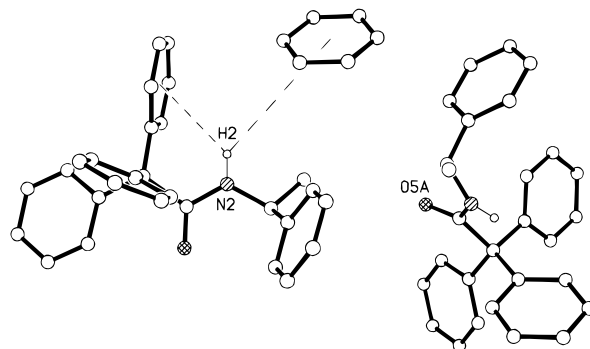


**Figure 3.** Ball-and-stick representation of the neighboring pair of molecules in crystalline **4** with shortest intermolecular NH···O separation (geometrical parameters may be found in Table II). The atoms of interest are labeled. The dotted lines indicate the shortest intramolecular and intermolecular NH···O (centroid) contacts in the crystal.

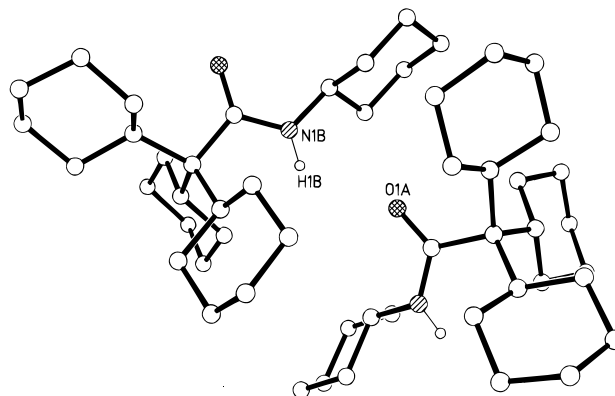


**Figure 4.** Ball-and-stick representation of the neighboring pair of molecules in crystalline **6** with the shortest intermolecular NH···O separation (geometrical parameters may be found in Table 2). The atoms of interest are labeled.

matic π-systems, and these interactions typically cause a shift in the N–H stretch band of 20–30 cm<sup>-1</sup> to lower energy.<sup>7</sup> It is therefore possible that amides **1–5** experience NH···π hydrogen bonding in solution and/or in the solid state, although the available data suggest that such interactions do not occur. Figure 2 shows that intramolecular NH···π hydrogen bonding in **1** involving the closest phenyl is unlikely, because this phenyl ring is constrained to lie approximately parallel to the N–H

bond axis, while NH- $\pi$  hydrogen bonding presumably requires a perpendicular orientation. Figure 3 leads to a similar conclusion regarding the closest phenyl on the carbonyl side of **4**; this view also shows that intramolecular NH- $\pi$  hydrogen bonding does not occur with the phenyl group on the nitrogen side. Figures 2 and 3 also display the shortest intermolecular N-H-phenyl interactions in crystalline **1** and **4**. The shortest intermolecular NH-C(aromatic) distance is 2.93 Å in crystalline **1**, and 3.56 Å in crystalline **4**. The former value is approximately equal to the sum of the hydrogen and aromatic carbon van der Waals radii,<sup>8</sup> and the latter is substantially larger than this sum. Thus, N-H-phenyl hydrogen bonding might occur in **1**, but not in **4**.

**Conclusions.** The IR and crystallographic data we have presented indicate that intermolecular hydrogen bonding is not obligatory among secondary amides derived from 2,2,2-triphenylacetic acid, or from the saturated analogue 2,2,2-tricyclohexylacetic acid. Although it is common to view intermolecular hydrogen bonds as crucial determinants of solid state packing,<sup>9</sup> most of the packing energy in molecules like **1–6** probably arises from dispersion interactions, and it may be energetically advantageous to forgo hydrogen bonds in favor of superior contact among hydrocarbon surfaces. The DMSO solution data indicate that hydrogen bond donation by **1–5** is sterically disfavored, a factor that must also contribute to the solid state packing behavior of these amides.

The indifference to solid state hydrogen bonding we observe among **1–6** may be a general feature of molecules that contain hydrogen bonding groups in sterically hindered environments. Ferguson et al., for example, have recently reported that there is no intermolecular OH-O hydrogen bonding in crystalline 1,1,2-triphenylethanol.<sup>10</sup> In this case, however, there is a well-developed OH- $\pi$  hydrogen bond in the solid state (OH-C(aromatic) distance = 2.73 Å), while NH- $\pi$  hydrogen bonding does not occur in crystalline **4** or **6**, and is possible but not certain in **1**. Amides **1–6** and related compounds should be useful for calibrating modern spectroscopic methods that are intended to provide insight on solid state hydrogen bonding.

## Experimental Section

Acid chlorides were prepared by refluxing the carboxylic acid in thionyl chloride for 3 h and removing the excess thionyl chloride under vacuum. THF was distilled from sodium and benzophenone under N<sub>2</sub>. Dry CH<sub>2</sub>Cl<sub>2</sub> was obtained by distillation from CaH<sub>2</sub> under N<sub>2</sub>. Triethylamine was distilled before use. The term "concentrated" below refers to concentration by rotary evaporation. Column chromatography was performed under low air pressure with use of 230–400 mesh silica gel 60 from EM Separations Technology. All melting points are uncorrected. NMR spectra were obtained on Bruker AM-500, AC-300, or AC-250 spectrometers. FT-IR spectra were obtained on a Nicolet 740 instrument. Solution IR samples were prepared under N<sub>2</sub> in a glovebag. High-resolution electron impact ionization mass spectrometry was performed with a Kratos MS-80.

**Amide 1** was prepared by the slow addition of 40% aqueous methylamine (10 mL, 14 mmol) to an ice cold solution of triphenylacetyl chloride (1.1 g, 3.5 mmol) in THF (50 mL). The solution was stirred for 30 min and then concentrated. The residue was redissolved in CH<sub>2</sub>Cl<sub>2</sub>, and the solution was washed with 1 M NaOH. The organic layer was dried with MgSO<sub>4</sub> and concentrated. Recrystallization from CH<sub>2</sub>Cl<sub>2</sub>/hexanes/ethanol gave a white flaky solid: mp 208–9 °C; <sup>1</sup>H NMR (CDCl<sub>3</sub>, 300 MHz)  $\delta$  2.85 (d, *J* = 4.8 Hz, 3 H), 5.81 (s, 1 H), 7.25 (m, 15 H); <sup>13</sup>C NMR (CDCl<sub>3</sub>, 75.4 MHz)  $\delta$  27.04, 67.75, 126.98,

127.90, 130.54, 143.49, 173.92; EI-MS *m/z* (M<sup>+</sup>) calcd for C<sub>21</sub>H<sub>19</sub>NO 301.1467, obsd 301.1480.

**Amide 2** was synthesized by adding benzylamine (0.23 mL, 2.06 mmol) to an ice cold mixture of triphenylacetyl chloride (0.60 g, 1.87 mmol) in THF (15 mL) and NaOH (0.37 g, 9.25 mmol) in water (15 mL). The mixture was warmed to room temperature overnight with stirring. The solution was then extracted with CH<sub>2</sub>Cl<sub>2</sub> and washed successively with 1 M NaOH, 1 M HCl, and water. The organic layer was dried with MgSO<sub>4</sub> and concentrated. Amide **2** was purified by recrystallization from hexanes/acetone to yield 0.53 g (1.4 mmol, 75%) of a white solid: mp 176–8 °C; <sup>1</sup>H NMR (CDCl<sub>3</sub>, 300 MHz)  $\delta$  4.52 (d, *J* = 5.7 Hz, 2 H), 6.09 (broad m, 1 H), 7.1–7.4 (m, 20 H); <sup>13</sup>C NMR (CDCl<sub>3</sub>, 75.4 MHz)  $\delta$  44.19, 67.80, 127.00, 127.36, 127.56, 127.94, 128.59, 130.52, 138.09, 143.34, 173.13; EI-MS *m/z* (M<sup>+</sup>) calcd for C<sub>27</sub>H<sub>23</sub>NO 377.1780, obsd 377.1797.

**Amide 3** was prepared and purified in an analogous manner in 74% yield: mp 170–2 °C; <sup>1</sup>H NMR (CDCl<sub>3</sub>, 300 MHz)  $\delta$  4.47 (d, *J* = 5.9 Hz, 2 H), 6.08 (broad m, 1 H), 7.0–7.4 (m, 19 H); <sup>13</sup>C NMR (CDCl<sub>3</sub>, 75.4 MHz)  $\delta$  43.28, 67.79, 126.87, 127.80, 128.51, 128.79, 130.27, 132.98, 136.50, 143.04, 173.04; EI-MS *m/z* (M<sup>+</sup>) calcd for C<sub>27</sub>H<sub>22</sub>NOCl 411.1390, obsd 411.1392.

**Amide 4** was prepared from an ice cold solution of triphenylacetyl chloride (1.1 g, 3.5 mmol) in THF (50 mL). Addition of triethylamine (0.53 mL, 3.8 mmol) was followed by the dropwise addition of (*S*)-(–)- $\alpha$ -methylbenzylamine (0.49 mL, 3.8 mmol). The solution was warmed to room temperature overnight with stirring. Aqueous 1 M NaOH (50 mL) was added, and the solution was concentrated and then extracted with CH<sub>2</sub>Cl<sub>2</sub>. The extract was washed with 1 M HCl, dried with MgSO<sub>4</sub>, and concentrated. Purification by recrystallization from CH<sub>2</sub>Cl<sub>2</sub>/hexanes gave 0.93 g (2.4 mmol, 68%) of colorless prisms: mp 100–101.5 °C; <sup>1</sup>H NMR (CDCl<sub>3</sub>, 300 MHz)  $\delta$  1.40 (d, *J* = 7.0 Hz, 3 H), 5.22 (dq, *J* = 7.3, 7.0 Hz, 1 H), 5.93 (d, *J* = 7.3, 1 H), 7.0–7.3 (m, 20 H); <sup>13</sup>C NMR (CDCl<sub>3</sub>, 75.4 MHz)  $\delta$  21.54, 49.31, 67.47, 125.81, 126.76, 127.05, 127.70, 128.36, 130.34, 142.87, 143.20, 171.97; EI-MS *m/z* (M<sup>+</sup>) calcd for C<sub>28</sub>H<sub>26</sub>NO 392.2014, obsd 392.2002.

**Amide 5** was prepared in a manner analogous to amide **2**. Amide **5** was purified by SiO<sub>2</sub> column chromatography eluting with CH<sub>2</sub>Cl<sub>2</sub> (*R*<sub>f</sub> 0.29) and recrystallization from methanol to yield 0.10 g (0.27 mmol, 15%) of white needles: mp 129–30 °C; <sup>1</sup>H NMR (CDCl<sub>3</sub>, 300 MHz)  $\delta$  0.9–1.9 (m, 10 H), 3.91 (m, 1 H), 5.62 (d, *J* = 8.1, 1 H), 7.26 (m, 15 H); <sup>13</sup>C NMR (CDCl<sub>3</sub>, 75.4 MHz)  $\delta$  24.34, 25.29, 32.41, 48.46, 67.42, 126.72, 127.64, 130.37, 143.35, 171.89; EI-MS *m/z* (M<sup>+</sup>) calcd for C<sub>26</sub>H<sub>28</sub>NO 370.2171, obsd 370.2163.

**Amide 6** was prepared from tricyclohexylacetyl chloride. Tricyclohexylacetic acid was prepared by a known procedure,<sup>11</sup> and the crude tricyclohexylacetic acid (0.10g, 0.33 mmol) was used to make the acid chloride. Tricyclohexylacetyl chloride was dissolved in dry CH<sub>2</sub>Cl<sub>2</sub> (25 mL) and cooled in an ice bath. Cyclohexylamine (0.19 mL, 1.7 mmol) was added dropwise, and the reaction mixture was stirred overnight and warmed to room temperature. The mixture was then refluxed for 1 h. The solution was washed successively with 1 M HCl, 1 M NaOH, and water. The organic layer was dried with MgSO<sub>4</sub> and concentrated. Compound **6** was purified by SiO<sub>2</sub> column chromatography eluting with CH<sub>2</sub>Cl<sub>2</sub> (*R*<sub>f</sub> 0.29) and recrystallization from methanol to afford 0.065 g (0.17 mmol, 11% from crude acid) of a white solid: mp 144–5 °C; <sup>1</sup>H NMR (CDCl<sub>3</sub>, 250 MHz)  $\delta$  1.0–2.0 (m, 43 H), 3.85 (m, 1 H), 5.35 (d, *J* = 9.8 Hz, 1 H); <sup>13</sup>C NMR (CDCl<sub>3</sub>, 125.8 MHz)  $\delta$  24.91, 25.71, 27.13, 28.41, 29.70, 33.39, 48.01, 57.14, 172.72; EI-MS *m/z* (M<sup>+</sup>) calcd for C<sub>26</sub>H<sub>48</sub>NO 387.3501, obsd 387.3486.

**IR Spectroscopy.** **1. Chloroform.** Chloroform was washed with water to remove the ethanol, dried by refluxing over CaH<sub>2</sub> overnight, distilled from CaH<sub>2</sub> onto activated 4 Å sieves, and stored in the dark under N<sub>2</sub> (glovebag). All spectra were acquired at a concentration of ca. 5 mM in a 1 mm path length CaF<sub>2</sub> cell. **2. DMSO.** DMSO was dried by storing over activated 4 Å sieves overnight followed by distillation under vacuum into a flask containing activated sieves. The sieves were then replaced successively for 2–3 days following

(8) Bondi, A. J. *Phys. Chem.* **1964**, *68*, 441.

(9) Desiraju, G. R. *Crystal Engineering. The Design of Organic Solids*; Elsevier: Amsterdam, 1989.

(10) Ferguson, G.; Gallagher, J. F.; Glidewell, C.; Zakaria, C. M. *Acta Crystallogr.* **1994**, *C50*, 70.

(11) Brian, E. G.; Doyle, F. P.; Hardy, K.; Long, A. A. W.; Mehta, M. D.; Miller, D.; Nayler, J. H. C.; Soulal, M. J.; Stove, E. R.; Thomas, G. R. *J. Chem. Soc.* **1962**, 1445.

distillation, and the bottle was stored under N<sub>2</sub> (glovebag). All spectra were acquired at a concentration of ca. 10 mM in a 0.1 mm path length CaF<sub>2</sub> cell.

**X-ray Crystallography.** X-ray quality crystals of amides **1** and **4** were obtained by the recrystallization methods given above. Crystals suitable for diffraction of **6** were obtained by slow evaporation of a solution of **6** in 1,2-dichloroethane. Data studies were obtained with a Siemens CCD X-ray diffraction system, and crystal temperature was maintained with a nitrogen cryostat. Phi scan frames with a 30 s/frame scan time were collected with use of Mo K $\alpha$  radiation. Data collection was carried out with the SMART software package, and the SAINT software package performed the data reduction. The structure was solved and refined by using the SHELXTL software package.

**Acknowledgment.** This research was supported by the National Science Foundation (CHE-9622653). D.T.M. is the recipient of a 1996–7 Fellowship from Pharmacia & Upjohn, awarded by the Organic Division of the American Chemical Society. S.L.M. is a fellow in the NIH CBI Training Program. S.H.G. is a Sloan Fellow. We thank NSF and NIH for support of the NMR facility (CHE-9208463 and 1 S10 RR08389) and NSF and the University of Wisconsin for support of the crystallography facility (CHE-9310428).

JA9711019